HHS Public Access

Author manuscript

Neurochem Int. Author manuscript; available in PMC 2017 June 01.

Published in final edited form as:

Neurochem Int. 2016 June ; 96: 24–31. doi:10.1016/j.neuint.2016.04.006.

Class IIa Histone Deacetylases Affect Neuronal Remodeling and Functional Outcome after Stroke

Haifa Kassis, MD[1,2], **Amjad Shehadah, MD**[1,3], **Chao Li, PhD**[1], **Yi Zhang, PhD**[1], **Yisheng Cui, MD**[1], **Cynthia Roberts, BS**[1], **Neema Sadry, BS**[1], **Xianshuang Liu, MD, PhD**[1], **Michael Chopp, PhD**[1,4], and **Zheng Gang Zhang, MD, PhD**[1]

[1]Department of Neurology, Henry Ford Health System, Detroit, MI 48202

[4]Department of Physics, Oakland University, Rochester, MI 48309

Abstract

We have previously demonstrated that stroke induces nuclear shuttling of class IIa histone deacetylase 4 (HDAC4). Stroke-induced nuclear shuttling of HDAC4 is positively and significantly correlated with improved indices of neuronal remodeling in the peri-infarct cortex. In this study, using a rat model for middle cerebral artery occlusion (MCAO), we tested the effects of selective inhibition of class IIa HDACs on functional recovery and neuronal remodeling when administered 24hr after stroke. Adult male Wistar rats (n = 15–17/group) were subjected to 2h MCAO and orally gavaged with MC1568 (a selective class IIa HDAC inhibitor), SAHA (a non-selective HDAC inhibitor), or vehicle-control for 7 days starting 24h after MCAO. A battery of behavioral tests was performed. Lesion volume measurement and immunohistochemistry were performed 28 days after MCAO. We found that stroke increased total HDAC activity in the ipsilateral hemisphere compared to the contralateral hemisphere. Stroke-increased HDAC activity was significantly decreased by the administration of SAHA as well as by MC1568. However, SAHA significantly improved functional outcome compared to vehicle control, whereas selective class IIa inhibition with MC1568 increased mortality and lesion volume and did not improve functional outcome. In addition, MC1568 decreased microtubule associated protein 2 (MAP2, dendrites), phosphorylated neurofilament heavy chain (pNFH, axons) and myelin basic protein (MBP, myelination) immunoreactivity in the peri-infarct cortex. Quantitative RT-PCR of cortical neurons isolated by laser capture microdissection revealed that MC1568, but not SAHA, downregulated CREB and c-fos expression. Additionally, MC1568 decreased the expression of phosphorylated CREB (active) in neurons. Taken together, these findings demonstrate that selective inhibition of class IIa HDACs impairs neuronal remodeling and neurological outcome. Inactivation of CREB and c-fos by MC1568 likely contributes to this detrimental effect.

Please send all correspondence to: Zheng Gang Zhang, MD, Ph.D, Department of Neurology, Henry Ford Hospital, 2799 West Grand Boulevard, Detroit, MI 48202, Tel: 1-313-916-5456, Fax: 1-313-916-1318, zhazh@neuro.hfh.edu.

[2]current address: Uniformed Services University of the Health Sciences, Department of Pharmacology and Molecular Therapeutics, Bethesda, MD 20814

[3]current address: Section on Stroke Diagnostics and Therapeutics, National Institute of Neurological Disorders and Stroke, Bethesda, MD 20892

Keywords

Epigenetics; Stroke; Neuronal repair

Introduction

Each year, nearly 800,000 people experience a new or recurrent stroke in the United States (Mozaffarian et al., 2015). Long-term disability and institutionalization are common sequelae among survivors of stroke, affecting one third and one seventh of patients, respectively (Hankey et al., 2002). Thus, a tremendous need exists for the development of new effective therapies that could potentially improve neurological outcome.

Histone acetylation is a major epigenetic regulatory mechanism implicated in a large number of neuropathological conditions ranging from Huntington's disease (Steffan et al., 2001), amyotrophic lateral sclerosis (Ryu et al., 2005), Parkinson's disease (Gardian et al., 2004) and Stroke (Faraco et al., 2006; Kim et al., 2007; Ren et al., 2004).

Histone deacetylases (HDACs) are a large family of enzymes that deacetylate lysine residues in histone tails, which leads to condensation of chromatin and gene repression. HDACs have recently emerged as a potential therapeutic target for stroke (Langley et al., 2009). HDACs are classified into four major classes based on homology to yeast enzymes (de Ruijter et al., 2003). Class I HDACs are Rpd3-like proteins and include HDACs 1, 2, 3 and 8. Class II HDACs are Hda1-like proteins and include HDACs 4, 5, 6, 7, 9 and 10. Based on their structure, class II HDACs are further subdivided into two subclasses: class IIa (4, 5, 7 and 9) and class IIb HDACs (6 and 10).

Many non-selective HDAC inhibitors such as valproic acid (VPA), suberoylanilide hydroxamic acid (SAHA), 4-phenylbutyrate and trichostatin A (Faraco et al., 2006; Gibson and Murphy, 2010; Kim et al., 2007; Qi et al., 2004; Ren et al., 2004) have been tested in experimental stroke models and were shown to induce neuroprotection and reduce inflammation when administered within a few hours after stroke onset. However, in contrast to their roles in neuroprotection, the effects of HDAC inhibitors on neuronal remodeling and recovery after ischemia have not been extensively studied.

Within days after an ischemic event, processes of neuronal remodeling such as axonal sprouting and formation of new cortical connections are induced in the areas adjacent to the infarct border and may contribute to spontaneous functional improvement after stroke (Carmichael et al., 2001; Dancause et al., 2005; Liu et al., 2009b). We have previously demonstrated that stroke induces diverse changes in the expression profiles as well as the subcellular localizations of individual HDAC isoforms in the peri-infarct white and grey matter during brain repair after ischemic injury (Kassis et al., 2014; Kassis et al., 2015).

The vast majority of HDAC-targeting drugs that were previously tested in experimental stroke models are broad non-selective HDAC inhibitors (Faraco et al., 2006; Kim et al., 2007; Qi et al., 2004; Ren et al., 2004). Subsequently, the identity of the specific HDAC classes that may mediate a therapeutic effect in stroke remains unknown (Chuang et al.,

2009). Interestingly, when the selective class I HDAC inhibitor MS-275 was tested *in vivo* and *in vitro*, it was found to be protective to both white and gray matter (Gibson and Murphy, 2010; Murphy et al., 2014). However, selective class IIa HDAC inhibitors have not been previously tested in a stroke model. Class IIa HDACs 4 and 5 are highly expressed in the cytoplasm of brain cells under physiological conditions (Darcy et al., 2010). We found that stroke induces a robust increase in nuclear shuttling of HDAC4 in cortical neurons of the peri-infarct cortex during stroke recovery (Kassis et al., 2015). HDAC4 and HDAC5 are highly similar in structure (70% homology). Stroke-induced shuttling of class IIa HDACs is specific to HDAC4 and is not observed with HDAC5, suggesting the existence of specific roles for the individual HDAC isoforms in mediating ischemic brain repair processes. Stroke-induced nuclear shuttling of HDAC4 in neurons is positively and significantly correlated with improved indices of neuronal remodeling in the ischemic cortex (Kassis et al., 2015). Based on these data, we hypothesized that class IIa HDACs can be beneficial for endogenous neuronal remodeling and functional recovery after stroke, and selective inhibition of class IIa HDACs may have a detrimental effect on brain repair after stroke. To test this hypothesis, we employed a rat model of focal cerebral ischemia to examine the effects of MC1568; a selective class IIa HDAC inhibitor (Mai et al., 2005; Nebbioso et al., 2009) on functional outcome and neuronal remodeling after stroke. We also tested whether SAHA; a non-selective HDAC inhibitor (Huber et al., 2011; Lauffer et al., 2013) improves functional recovery when administered 24 hours after stroke.

Materials and Methods

This study was carried out in strict accordance with the recommendations in the Guide for the Care and Use of Laboratory Animals of the National Institutes of Health. All experimental procedures have been approved by the Institutional Animal Care and Use Committee (IACUC) of Henry Ford Health System.

Drug preparation

HDAC inhibitors—MC1568 (selective class IIa HDAC inhibitor) and SAHA (non-selective HDAC inhibitor) were purchased from Selleck Chemicals. Before each administration, the drugs were freshly dissolved in a water solution of low-viscosity 0.5% carboxymethyl cellulose (Spectrum Chemical Mfg. Corp.), as previously described (Nebbioso et al., 2010).

Animal Model for Stroke

Adult male Wistar rats (270–300 g, 2–3 months, Charles River Breeding Company) were subjected to 2 hours of transient right middle cerebral artery occlusion (MCAO) using a method of intraluminal vascular occlusion modified in our laboratory (Chen et al., 1992; Zhang et al., 2009). Briefly, following anesthesia with isoflurane and nitrous oxide, neck dissection was performed to expose the right common carotid artery (CCA), the right external carotid artery (ECA) and the internal carotid artery (ICA). A 4-0 surgical nylon suture (18.5–19.5 mm, as determined by the animal's weight) with an expanded tip was then advanced from the right ECA into the lumen of the ICA to block the origin of the MCA. Reperfusion was performed by withdrawal of the suture 2 hours after MCAO.

Experimental Groups

Adult male Wistar rats were subjected to MCAO and 24 hours after surgery were randomly divided into three groups: 1) Non-selective HDAC inhibitor group (SAHA-treated group, n=17): rats were daily gavaged with 1.5 mL of SAHA at 25 mg/kg for 7 days. 2) Class IIa HDAC selective inhibitor group (MC1568-treated, n=15): rats were gavaged with 1.5 mL of MC1568 at 25 mg/kg every 2 days for 7 days (Mannaerts et al., 2013; Nebbioso et al., 2009). 3) Control: (vehicle-treated group, n=15): rats were daily gavaged with 1.5 mL of 0.5% carboxymethyl cellulose (CMC) for 7 days. Rats were sacrificed 28 days after MCAO.

MC1568 is a selective class IIa HDAC inhibitor and not specific for HDAC4. We chose to use this compound after extensive search of the commercially available HDAC inhibitors. None of the other available HDAC inhibitors was shown to be more specific for class IIa HDAC.

Functional Testing

All functional tests were performed by an investigator adequately trained in functional measurements and blinded to the experimental groups. All rats were familiarized with the testing environment before surgery and were returned to their home cages after each testing session. Functional tests were performed prior to initiating therapy 1 day after MCAO and 7, 14, 21 and 28 days after MCAO. Animals that died during the course of treatment were excluded from the behavioral tests. Subsequently, the numbers of animals used for the behavioral tests in each group were: vehicle-control group (n=13); MC1568 group (n=10); SAHA group (n=14).

Foot-fault test—This test assesses placement dysfunction of forelimbs (Barth et al., 1990). Rats were placed on an elevated grid floor (45 cm×30 cm), 2.5 cm higher than a solid base floor, with 2.5 cm×2.5 cm diameter openings. Animals tend to move on the grid with their paws placed on the wire frame. When animals inaccurately place a paw, the front limb falls through one of the openings in the grid. When the paw falls through or slips between the wires, it is recorded as a foot fault. A total of 100 steps (movements of each forelimb) were counted, and the total number of foot faults for the left forelimb was recorded. The percentage of foot faults of the left paw out of total steps was calculated.

Modified neurological severity score (mNSS)—The mNSS is a composite of motor (muscle status, abnormal movement), sensory (visual, tactile, proprioceptive), reflex, and balance tests (Li et al., 2002) and is scored on a scale of 0 to 18 (normal score 0; maximal deficit score 18). One score point is awarded for the inability to perform the test or for the lack of a tested reflex; thus, a higher score indicates a more severe injury.

Tissue preparation for Immunohistochemistry

Twenty-eight days after MCAO, rats were re-anesthetized with Ketamine (80 mg/kg) and Xylazine (13 mg/kg) via i.p. injection. The animals were then subjected to cardiac puncture with saline perfusion (approximately 200 mL/rat) followed by perfusion with 4% paraformaldehyde (approximately 50 mL/rat). Brains were isolated and the cerebral

hemispheres were cut into seven equally spaced (2 mm) coronal blocks and embedded in paraffin.

Lesion Volume Measurement

Paraffin coronal sections (6 μm thick) from each of the 2 mm blocks were obtained and stained with Hematoxylin and Eosin (H&E) for calculation of lesion volume (Swanson et al., 1990). Each H&E stained coronal section was digitized under a 2.5× objective of a light microscope using micro computer imaging device (MCID) analysis system (Imaging Research Inc.). The area of infarction and the area of both hemispheres (mm^2) were calculated by tracing these areas on a computer screen. Volumes (mm^3) were determined by integrating the appropriate area with sections interval thickness. To reduce errors associated with processing of infarcted tissue for histology, the infarct volume was calculated as the percentage of infarct volume out of the volume of the contralateral hemisphere (indirect lesion volume) (Zhang et al., 1997).

Immunohistochemistry

A series of coronal sections (6 μm thick) were obtained at the center of the lesion, corresponding to coronal coordinates for Bregma −1 to +1 mm (Paxinos and Watson, 2007). Three coronal sections were used for each immunohistochemistry experiment per rat. The following primary antibodies were used: mouse anti-microtubule-associated protein 2 (neuronal somatodendritic marker, MAP2; 1:400, Millipore), mouse anti-phosphorylated neurofilament heavy chain (axonal marker, p-NFH; 1:500, Covance), rabbit anti-myelin basic protein (MBP; 1:400, Dako) and mouse anti-phosphorylated cAMP responsive element binding protein (p-CREB, 1:200, Abcam). Brain sections were incubated with the primary antibodies listed above and with Cy3 or FITC (Jackson ImmunoResearch) conjugated secondary antibodies. Control experiments consisted of staining brain coronal tissue sections as outlined above, but omitting the primary antibodies. Counterstaining with DAPI (4′,6-diamidino-2-phenylindole, Vector Laboratories) allowed visualization of cells nuclei.

Image acquisition and analysis

For quantification, coronal sections were digitized under a 20× objective of an epifluorescence microscope (Axiophot, Carl Zeiss Inc.) via an MCID imaging system (Imaging Research Inc.). Four-six fields of view were acquired from the peri-infarct sensorimotor cortex (up to 500 μm from the lesion border, Figure 3A). Immunoreactive cells were counted using NIH ImageJ software and immunoreactive areas were calculated using MCID imaging analysis system. Laser-scanning confocal microscopy (Zeiss LSM 510 NLO, Carl Zeiss Inc.) was used for three dimensional imaging.

HDAC activity assay

To examine the effects of SAHA and MC1568 treatments on HDAC catalytic activity in the ischemic brain, another set of adult male Wistar rats were subjected to MCAO (3 groups, n=6/group). Rats were gavaged with either SAHA (25 mg/kg/d), MC1568 (25 mg/kg/2d) or vehicle (0.5% CMC) for 7 days starting 1 day after stroke. Seven days after MCAO at 2 hours after the last gavage, rats were re-anesthetized with Ketamine (80 mg/kg) and

Xylazine (13 mg/kg) via i.p. injection and subjected to cardiac puncture with saline perfusion (approximately 200 mL per rat). Brains were isolated, embedded in cryoprotective OCT solution and flash frozen in 2-methyl butane on dry ice and then stored at −80°C.

A series of cryosections (25 μm thick) were obtained at the center of the lesion, corresponding to coronal coordinates for Bregma −1 to +1 mm (Paxinos and Watson, 2007), and used for protein isolation. Nuclear extracts were prepared using BioVision Nuclear/Cytosol Fractionation Kit (Catalog #K266-25) following the manufacturer's manual. Protein concentrations were determined by a Pierce™ BCA Protein Assay Kit following the protocol provided by the manufacturer (Life Technologies). HDAC activity was measured on 80 μg of nuclear extract from each sample using a BioVision HDAC activity Colorimetric Assay Kit (Catalog #K331). Samples were read in an ELISA plate reader at 405 nm. HDAC activity is presented as absolute optical density (OD) values obtained from equal amounts of nuclear extracts.

Laser Capture micro-dissection (LCM)

Coronal cryosections (10 μm) were obtained at the center of the lesion (Bregma −1 to +1 mm) from frozen brains of SAHA-treated, MC1568-treated and vehicle-control rats that were sacrificed 7 days after MCAO. Sections were mounted on polyethylene naphthalate (PEN) membrane slides (Leica Microsystems). To identify neurons, frozen sections were stained with a neuronal specific anti-NeuN antibody using a fast immunostaining protocol, as previously described (Liu et al., 2009a). Briefly, frozen brain coronal sections were air-dried for 30s at room temperature and then immersed in ice-cold acetone for 2 min of fixation. After a brief rinse with 0.1% diethylpyrocarbonate-treated phosphate buffered saline (DEPC-PBS), sections were stained with a mouse anti-NeuN antibody (Millepore, 1:50 dilution) for 5 min followed by a Cy3-conjugated secondary antibody (DAKO, 1:50 dilution) for 5 min. After a brief rinse with DEPC-PBS, sections were air-dried under laminar flow for 10 min and immediately used for LCM. Approximately 2,000 NeuN positive neurons were quickly collected from the peri-infarct cortex of each animal using a Leica LMD6000 Microsystem (Figure 4A).

Isolation of total RNA and real-time RT-PCR

LCM captured neurons were collected in Qiazol lysis reagent (Qiagen). Total RNA was isolated using the miRNeasy Mini Kit (Qiagen). RNA was reverse transcribed with SuperScript® III Reverse Transcriptase (Life Technologies) and amplified with SYBR Green reporter (Applied Biosystems) using custom made primers (Invitrogen). Quantitative RT-PCR was performed on a ViiA™ 7 Real-Time PCR System (Life Technologies).

To verify the purity of neurons isolated by LCM, mRNA levels of MAP2 (a marker for neurons) and glial fibrillary protein (GFAP, a marker for astrocytes) were measured. Real-time RT-PCR analysis showed the presence of MAP2 mRNA, but not GFAP transcripts in the cells, indicating that the collected cells are cerebral neuronal cells. After the verification, we then examined mRNA expression for CREB and c-FOS. The following primers were employed: GAPDH: 5′-AGAGAGAGGCCCTCAGTTGCT-3′ (forward), 5′-TTGTGAGGGAGATGCTCAGTGT-3′ (reverse), CREB: 5′-

CTGATTCCCAAAAACGAAGG-3′ (forward), 5′-CTGCCCACTGCTAGTTTGGT-3′ (reverse), c-fos: 5′-TTTCAACGCGGACTACGAGG-3′ (forward), 5′-GCGCAAAAGTCCTGTGTGTT-3′ (reverse), MAP2: 5′-CAGAACATACCACCAGCCCT-3′ (forward), 5′-TGAGTGAGGCTGATGTCCAG-3′ (reverse) and GFAP: 5′-GGTGGAGAGGGACAATCTCA-3′ (forward), 5′-ACACAGCCAGGTTGTTCTCC-3′ (reverse). Specificity of the produced amplification product was confirmed by examination of dissociation reaction plots. Samples (n=3/group) were used for analysis of relative gene expression using the $2^{-\Delta\Delta CT}$ method (Livak and Schmittgen, 2001).

Statistical Analysis

Student's t test analysis was used for two group comparison. One-way analysis of variance (ANOVA) with post hoc Bonferroni test was used for data analysis of multiple group experiments. Chi-Square test was done to compare the mortality rate. Repeated measure analysis of variance (ANOVA) was performed for functional tests. Statistical significance was set at p-value <0.05. All values are presented as mean ± SE for illustration.

Results

Nuclear HDAC Activity in the Ischemic Brain in vivo

To verify the inhibitory effects of MC1568 and SAHA on HDAC catalytic activity in the ischemic brain *in vivo*, a cohort of adult male Wistar rats (n=6/group) were subjected to MCAO and treated with either MC1568, SAHA or vehicle for 1 week. Sham rats were used for control. Rats were sacrificed 7 days after MCAO, 2 hours after the last dose. Equal amounts of nuclear protein were isolated from ipsilateral and contralateral cerebral hemispheres to test total HDAC activity in nuclei of brain cells. We found that levels of HDAC activity were relatively the same in both hemispheres of sham operated rats (0.31 ± 0.006 in ipsilateral vs. 0.32 ± 0.009 in contralateral, p>0.05) and that those levels were comparable to HDAC activity in the contralateral hemisphere of ischemic rats in the vehicle-control group (0.32 ± 0.016, p>0.05).

In vehicle-control rats, stroke significantly (p<0.05) increased HDAC activity in the ipsilateral hemisphere compared with the contralateral hemisphere (~2 fold, Figure 1A) which is consistent with previous studies that reported reduced global histone acetylation levels in the brains of rodents after focal ischemia (Faraco et al., 2006; Kim et al., 2007; Ren et al., 2004). Stroke-increased HDAC activity in the ipsilateral hemisphere was significantly decreased by the administration of SAHA (~0.6 fold, Figure 1B), as well as by MC1568 (~0.75 fold, Figure 1B). These experiments show that stroke induces an increase in HDAC activity in the ischemic brain and administration of MC1568 and SAHA at the doses used in our experimental protocols block the increased HDAC activity in the ischemic brain *in vivo*.

Neurological Outcome and Lesion Volume

To examine the effects of selective and non-selective HDAC inhibition on neurological outcome after stroke, rats were subjected to 2 hour transient MCAO and behavioral tests

were performed one day after MCAO just prior to randomization and initiation of treatments. Behavioral testing was repeated thereafter weekly for a total of 4 weeks.

Analysis of foot-fault and mNSS tests revealed that non-selective HDAC inhibition with SAHA significantly improved functional outcome (Figure 2A–B, $p<0.05$ vs. vehicle-control group) at 21 and 28 days after stroke, whereas selective class IIa HDAC inhibition with MC1568 did not result in functional improvement after stroke. On the contrary, the mortality rate in the MC1568-treated group was significantly higher than the mortality rate in the vehicle-control and SAHA groups (Figure 2C, $p<0.05$). Animals in the MC1568-treatment group were found dead mainly between 3 and 5 days after MCAO and autopsy revealed large infarcts with signs of edema in the brains of these rats. Furthermore, quantification showed that MC1568 administration significantly ($p<0.05$) increased the ischemic lesion volumes compared with the vehicle-control and SAHA groups 28 days after MCAO (42.8% ± 2.7 in MC1568-treated group vs. 35% ± 2.1 in vehicle-control group and 32.37% ± 3.2 SAHA-treated group, Figure 2D). While SAHA administration starting 24 hours after MCAO improved functional outcome, it did not significantly reduce lesion volume compared to vehicle control ($p> 0.05$, Figure 2D).

Together, these data show that non-selective HDAC inhibition with SAHA improves neurological outcome when administered 24 hours after stroke, while selective inhibition of class IIa HDACs with MC1568 increases mortality and lesion volume with no beneficial effect on functional outcome.

MC1568, but not SAHA, Reduces Dendritic, Axonal and Myelination Densities during Brain Recovery after Stroke

Neuronal remodeling such as rewiring neuronal circuitry and re-myelination occurs in peri-infarct region during stroke recovery (Gensert and Goldman, 1997; Liu et al., 2009b). Thus, to examine the effects of selective and non-selective HDAC inhibition on neuronal remodeling after ischemia, we performed immunofluorescent staining for MAP2 (an index of dendrites), pNFH (a marker of axons) and MBP (an index of myelination). While non-selective HDAC inhibition with SAHA significantly increased MAP2 and pNFH densities in the peri-infarct cortex compared to vehicle-control, selective class IIa HDAC inhibition with MC1568 significantly decreased MAP2, pNFH and MBP densities in the peri-infarct cortex compared to vehicle-control ($p<0.05$, Figure 3B–D). These data clearly indicate detrimental effects for selective class IIa HDAC inhibition on neuronal repair processes after ischemic injury.

MC1568 Down-regulates, while SAHA Up-regulates CREB and c-fos in the Ischemic Cortex

CREB is a transcription factor induced by elevation in calcium concentration or cytoplasmic cAMP (Kristian and Siesjo, 1998). Stroke induces robust phosphorylation of CREB in the peri-infarct region (Tanaka et al., 1999) and activation of CREB leads to upregulation of the neuronal pro-survival gene c-fos (Kitagawa, 2007; Sugiura et al., 2004). To examine the effects of selective and non-selective HDAC inhibition on expression of CREB and c-fos after stroke, NeuN-positive neurons were captured from the peri-infarct cortex of vehicle,

MC1568 and SAHA-treated animals and evaluated by quantitative RT-PCR for CREB and c-fos genes.

While non-selective HDAC inhibition with SAHA significantly upregulated CREB and c-fos mRNAs in the peri-infarct cortex compared to vehicle-control, selective class IIa HDAC inhibition with MC1568 significantly downregulated both CREB and c-fos expression (Figure 4B–C). Furthermore, using double immunohistochemistry for phosphorylated CREB and MAP2, we found that MC1568 administration significantly decreased phosphorylated (active) CREB levels in neurons localized to the peri-infarct cortex (33.8 ± 7.4% in MC1568-treated group vs. 55.8 ± 5.4% in vehicle-control, $p<0.05$, Figure 4D). Together, these data show that MC1568 inactivates neuronal CREB and c-fos in ischemic brain.

Discussion

In the present study, we show for the first time that selective inhibition of class IIa HDACs impairs behavioral outcome and neuronal remodeling after stroke *in vivo*, suggesting that class IIa HDACs affect neuronal repair and functional outcome after ischemic injury.

Previous reports have demonstrated a dramatic decrease in histone acetylation levels in the ischemic brain that could last up to 14 days after stroke (Kim et al., 2009; Ren et al., 2004), however, direct measurement of HDAC catalytic activity in brain tissue was not extensively explored. To our knowledge, only one study tested HDAC activity after stroke and found that HDAC activity does not change during the first 6 hours after ischemia (Faraco et al., 2006). Here, our data show a robust increase in HDAC activity in the ipsilateral hemisphere of the brain compared with the contralateral hemisphere 7 days after stroke, indicating that an endogenous upregulation of HDAC activity occurs within days after stroke during the time period of brain repair after injury.

MC1568 is a selective class IIa histone deacetylase inhibitor with IC50 of 220 nM that displays no inhibition of class I HDAC activity or expression (Nebbioso et al., 2009). SAHA is a non-selective HDAC inhibitor with IC50 of 4.8–10 μM against class I HDACs with little to no inhibitory effect on class IIa HDACs (Kilgore et al., 2010). SAHA as well as MC1568 significantly reduce stroke-increased total HDAC activity, suggesting an upregulation of the activity of both class I and class II HDACs in nuclei of brain cells after stroke. Our data show that SAHA administration significantly improves behavioral functional outcome compared to vehicle control, while MC1568, the class IIa-selective inhibitor, increases mortality, lesion volume and worsened outcome. The differential effects of selective and non-selective HDAC inhibitors on outcome may be related to the minimal inhibition of class IIa HDACs by SAHA.

A promising approach to improve outcome during stroke recovery is to enhance the brain's intrinsic capability to facilitate brain repair processes including axonal sprouting and myelination after ischemia (Benowitz and Carmichael, 2010; Zhang and Chopp, 2009). Using immuohistochemsitry for MAP2, p-NFH, and MBP to determine dendritic, axonal, and myelin recovery, respectively, we found that non-selective HDAC inhibition with SAHA significantly increase neuronal neurite growth in the peri-infarct cortex compared to the

vehicle-control, while selective class IIa HDAC inhibition with MC1568 significantly reduce MAP2, pNFH and MBP densities. These data further support our hypothesis that class IIa HDACs may mediate brain repair after ischemic injury. Our previous study showed that HDAC4 shuttles to the nuclei only in neurons and that stroke does not change profiles of HDAC4 and 5 in oligodendrocytes. Therefore, we speculate that myelin loss is secondary to neuronal death. We have performed TUNEL assay for identification of apoptotic cells, however, since the animals were sacrificed 28 days after stroke which is too late for detecting the majority of apoptotic cells, few apoptotic cells were detected for statistical analysis. Subsequently, we were not able to determine if oligodendrocytes also die after MC1568 treatment.

Activation of CREB promotes axonal growth (Hannila and Filbin, 2008) and the CREB-binding protein regulates acetylation and deacetylation of transcription genes (Dai et al., 2015). Furthermore, the c-fos gene is a reliable indicator for neural activity (Morgan and Curran, 1991). Our data demonstrate that non-selective HDAC inhibition with SAHA significantly activated neuronal CREB and upregulated c-fos expression in the peri-infarct cortex, whereas selective class IIa HDAC inhibition with MC1568 substantially inactivated CREB and downregulated c-fos in neurons. Others have shown that stroke induces robust phosphorylation of CREB in the peri-infarct region (Tanaka et al., 1999). Collectively, our data along with published studies suggest that selective class IIa HDAC inhibition with MC1568 may inactivate neuronal CREB and thereby leads to impairment of axonal and dendritic sprouting and reduction of neuronal activity in peri-infarct cortex. Additional experiments to investigate whether overexpression of CREB in neurons will overcome the effect of MC1568 on ischemic lesion and neurite outgrowth are warranted.

In summary, our data suggest that class IIa HDACs are involved in brain remodeling and functional outcome after ischemic stroke. Inactivation of CREB may contribute to the detrimental effect of selective class IIa HDAC inhibition on neurons in the ischemic brain. Development of selective class IIa HDACs activators may represent a novel therapeutic approach that can potentially promote neuronal remodeling after brain injury even if administered days after stroke onset. Further studies are also needed to elucidate the roles of individual isoforms within the classes of HDACs on brain recovery after stroke.

Acknowledgments

This work was supported by NIH grants RO1 NS088656 (MC) and RO1 NS075156 (ZGZ). The content is solely the responsibility of the authors and does not necessarily represent the official view of the NIH. The authors wish to thank Qinge Lu and Sutapa Santra for technical assistance.

List of abbreviations

HDAC	histone deacetylase
MCAO	middle cerebral artery occlusion
SAHA	suberoylanilide hydroxamic acid
pNFH	phosphorylated neurofilament heavy chain

MBP	myelin basic protein
CREB	cAMP responsive element binding protein
mNSS	Modified neurological severity score
DAPI	4,6′-diamidino-2-phenylindole

References

Barth TM, Grant ML, Schallert T. Effects of MK-801 on recovery from sensorimotor cortex lesions. Stroke. 1990; 21:III153–157. [PubMed: 2237974]

Benowitz LI, Carmichael ST. Promoting axonal rewiring to improve outcome after stroke. Neurobiol Dis. 2010; 37:259–266. [PubMed: 19931616]

Carmichael ST, Wei L, Rovainen CM, Woolsey TA. New patterns of intracortical projections after focal cortical stroke. Neurobiol Dis. 2001; 8:910–922. [PubMed: 11592858]

Chen H, Chopp M, Zhang ZG, Garcia JH. The effect of hypothermia on transient middle cerebral artery occlusion in the rat. J Cereb Blood Flow Metab. 1992; 12:621–628. [PubMed: 1618941]

Chuang DM, Leng Y, Marinova Z, Kim HJ, Chiu CT. Multiple roles of HDAC inhibition in neurodegenerative conditions. Trends Neurosci. 2009; 32:591–601. [PubMed: 19775759]

Dai J, Bercury KK, Jin W, Macklin WB. Olig1 Acetylation and Nuclear Export Mediate Oligodendrocyte Development. J Neurosci. 2015; 35:15875–15893. [PubMed: 26631469]

Dancause N, Barbay S, Frost SB, Plautz EJ, Chen D, Zoubina EV, Stowe AM, Nudo RJ. Extensive cortical rewiring after brain injury. J Neurosci. 2005; 25:10167–10179. [PubMed: 16267224]

Darcy MJ, Calvin K, Cavnar K, Ouimet CC. Regional and subcellular distribution of HDAC4 in mouse brain. J Comp Neurol. 2010; 518:722–740. [PubMed: 20034059]

de Ruijter AJ, van Gennip AH, Caron HN, Kemp S, van Kuilenburg AB. Histone deacetylases (HDACs): characterization of the classical HDAC family. Biochem J. 2003; 370:737–749. [PubMed: 12429021]

Faraco G, Pancani T, Formentini L, Mascagni P, Fossati G, Leoni F, Moroni F, Chiarugi A. Pharmacological inhibition of histone deacetylases by suberoylanilide hydroxamic acid specifically alters gene expression and reduces ischemic injury in the mouse brain. Mol Pharmacol. 2006; 70:1876–1884. [PubMed: 16946032]

Gardian G, Yang L, Cleren C, Calingasan NY, Klivenyi P, Beal MF. Neuroprotective effects of phenylbutyrate against MPTP neurotoxicity. Neuromolecular Med. 2004; 5:235–241. [PubMed: 15626823]

Gensert JM, Goldman JE. Endogenous progenitors remyelinate demyelinated axons in the adult CNS. Neuron. 1997; 19:197–203. [PubMed: 9247275]

Gibson CL, Murphy SP. Benefits of histone deacetylase inhibitors for acute brain injury: a systematic review of animal studies. J Neurochem. 2010; 115:806–813. [PubMed: 20831615]

Hankey GJ, Jamrozik K, Broadhurst RJ, Forbes S, Anderson CS. Long-term disability after first-ever stroke and related prognostic factors in the Perth Community Stroke Study, 1989–1990. Stroke. 2002; 33:1034–1040. [PubMed: 11935057]

Hannila SS, Filbin MT. The role of cyclic AMP signaling in promoting axonal regeneration after spinal cord injury. Exp Neurol. 2008; 209:321–332. [PubMed: 17720160]

Huber K, Doyon G, Plaks J, Fyne E, Mellors JW, Sluis-Cremer N. Inhibitors of histone deacetylases: correlation between isoform specificity and reactivation of HIV type 1 (HIV-1) from latently infected cells. J Biol Chem. 2011; 286:22211–22218. [PubMed: 21531716]

Kassis H, Chopp M, Liu XS, Shehadah A, Roberts C, Zhang ZG. Histone deacetylase expression in white matter oligodendrocytes after stroke. Neurochem Int. 2014; 77:17–23. [PubMed: 24657831]

Kassis H, Shehadah A, Chopp M, Roberts C, Zhang ZG. Stroke Induces Nuclear Shuttling of Histone Deacetylase 4. Stroke. 2015; 46:1909–1915. [PubMed: 25967576]

Kilgore M, Miller CA, Fass DM, Hennig KM, Haggarty SJ, Sweatt JD, Rumbaugh G. Inhibitors of class 1 histone deacetylases reverse contextual memory deficits in a mouse model of Alzheimer's disease. Neuropsychopharmacology. 2010; 35:870–880. [PubMed: 20010553]

Kim HJ, Leeds P, Chuang DM. The HDAC inhibitor, sodium butyrate, stimulates neurogenesis in the ischemic brain. J Neurochem. 2009; 110:1226–1240. [PubMed: 19549282]

Kim HJ, Rowe M, Ren M, Hong JS, Chen PS, Chuang DM. Histone deacetylase inhibitors exhibit anti-inflammatory and neuroprotective effects in a rat permanent ischemic model of stroke: multiple mechanisms of action. J Pharmacol Exp Ther. 2007; 321:892–901. [PubMed: 17371805]

Kitagawa K. CREB and cAMP response element-mediated gene expression in the ischemic brain. FEBS J. 2007; 274:3210–3217. [PubMed: 17565598]

Kristian T, Siesjo BK. Calcium in ischemic cell death. Stroke. 1998; 29:705–718. [PubMed: 9506616]

Langley B, Brochier C, Rivieccio MA. Targeting histone deacetylases as a multifaceted approach to treat the diverse outcomes of stroke. Stroke. 2009; 40:2899–2905. [PubMed: 19478231]

Lauffer BE, Mintzer R, Fong R, Mukund S, Tam C, Zilberleyb I, Flicke B, Ritscher A, Fedorowicz G, Vallero R, Ortwine DF, Gunzner J, Modrusan Z, Neumann L, Koth CM, Lupardus PJ, Kaminker JS, Heise CE, Steiner P. Histone deacetylase (HDAC) inhibitor kinetic rate constants correlate with cellular histone acetylation but not transcription and cell viability. J Biol Chem. 2013; 288:26926–26943. [PubMed: 23897821]

Li Y, Chen J, Chen XG, Wang L, Gautam SC, Xu YX, Katakowski M, Zhang LJ, Lu M, Janakiraman N, Chopp M. Human marrow stromal cell therapy for stroke in rat: neurotrophins and functional recovery. Neurology. 2002; 59:514–523. [PubMed: 12196642]

Liu XS, Chopp M, Zhang RL, Hozeska-Solgot A, Gregg SC, Buller B, Lu M, Zhang ZG. Angiopoietin 2 mediates the differentiation and migration of neural progenitor cells in the subventricular zone after stroke. J Biol Chem. 2009a; 284:22680–22689. [PubMed: 19553662]

Liu Z, Zhang RL, Li Y, Cui Y, Chopp M. Remodeling of the corticospinal innervation and spontaneous behavioral recovery after ischemic stroke in adult mice. Stroke. 2009b; 40:2546–2551. [PubMed: 19478220]

Livak KJ, Schmittgen TD. Analysis of relative gene expression data using real-time quantitative PCR and the 2(-Delta Delta C(T)) Method. Methods. 2001; 25:402–408. [PubMed: 11846609]

Mai A, Massa S, Pezzi R, Simeoni S, Rotili D, Nebbioso A, Scognamiglio A, Altucci L, Loidl P, Brosch G. Class II (IIa)-selective histone deacetylase inhibitors. 1. Synthesis and biological evaluation of novel (aryloxopropenyl)pyrrolyl hydroxyamides. J Med Chem. 2005; 48:3344–3353. [PubMed: 15857140]

Mannaerts I, Eysackers N, Onyema OO, Van Beneden K, Valente S, Mai A, Odenthal M, van Grunsven LA. Class II HDAC inhibition hampers hepatic stellate cell activation by induction of microRNA-29. PLoS One. 2013; 8:e55786. [PubMed: 23383282]

Morgan JI, Curran T. Stimulus-transcription coupling in the nervous system: involvement of the inducible proto-oncogenes fos and jun. Annu Rev Neurosci. 1991; 14:421–451. [PubMed: 1903243]

Mozaffarian D, Benjamin EJ, Go AS, Arnett DK, Blaha MJ, Cushman M, de Ferranti S, Despres JP, Fullerton HJ, Howard VJ, Huffman MD, Judd SE, Kissela BM, Lackland DT, Lichtman JH, Lisabeth LD, Liu S, Mackey RH, Matchar DB, McGuire DK, Mohler ER 3rd, Moy CS, Muntner P, Mussolino ME, Nasir K, Neumar RW, Nichol G, Palaniappan L, Pandey DK, Reeves MJ, Rodriguez CJ, Sorlie PD, Stein J, Towfighi A, Turan TN, Virani SS, Willey JZ, Woo D, Yeh RW, Turner MB. American Heart Association Statistics, C., Stroke Statistics, S. Heart disease and stroke statistics--2015 update: a report from the American Heart Association. Circulation. 2015; 131:e29–322. [PubMed: 25520374]

Murphy SP, Lee RJ, McClean ME, Pemberton HE, Uo T, Morrison RS, Bastian C, Baltan S. MS-275, a class I histone deacetylase inhibitor, protects the p53-deficient mouse against ischemic injury. J Neurochem. 2014; 129:509–515. [PubMed: 24147654]

Nebbioso A, Dell'Aversana C, Bugge A, Sarno R, Valente S, Rotili D, Manzo F, Teti D, Mandrup S, Ciana P, Maggi A, Mai A, Gronemeyer H, Altucci L. HDACs class II-selective inhibition alters nuclear receptor-dependent differentiation. J Mol Endocrinol. 2010; 45:219–228. [PubMed: 20639404]

Nebbioso A, Manzo F, Miceli M, Conte M, Manente L, Baldi A, De Luca A, Rotili D, Valente S, Mai A, Usiello A, Gronemeyer H, Altucci L. Selective class II HDAC inhibitors impair myogenesis by modulating the stability and activity of HDAC-MEF2 complexes. EMBO Rep. 2009; 10:776–782. [PubMed: 19498465]

Paxinos, G.; Watson, C. The rat brain in stereotaxic coordinates. 6. Academic Press/Elsevier; Amsterdam; Boston: 2007.

Qi X, Hosoi T, Okuma Y, Kaneko M, Nomura Y. Sodium 4-phenylbutyrate protects against cerebral ischemic injury. Mol Pharmacol. 2004; 66:899–908. [PubMed: 15226415]

Ren M, Leng Y, Jeong M, Leeds PR, Chuang DM. Valproic acid reduces brain damage induced by transient focal cerebral ischemia in rats: potential roles of histone deacetylase inhibition and heat shock protein induction. J Neurochem. 2004; 89:1358–1367. [PubMed: 15189338]

Ryu H, Smith K, Camelo SI, Carreras I, Lee J, Iglesias AH, Dangond F, Cormier KA, Cudkowicz ME, Brown RH Jr, Ferrante RJ. Sodium phenylbutyrate prolongs survival and regulates expression of anti-apoptotic genes in transgenic amyotrophic lateral sclerosis mice. J Neurochem. 2005; 93:1087–1098. [PubMed: 15934930]

Steffan JS, Bodai L, Pallos J, Poelman M, McCampbell A, Apostol BL, Kazantsev A, Schmidt E, Zhu YZ, Greenwald M, Kurokawa R, Housman DE, Jackson GR, Marsh JL, Thompson LM. Histone deacetylase inhibitors arrest polyglutamine-dependent neurodegeneration in Drosophila. Nature. 2001; 413:739–743. [PubMed: 11607033]

Sugiura S, Kitagawa K, Omura-Matsuoka E, Sasaki T, Tanaka S, Yagita Y, Matsushita K, Storm DR, Hori M. CRE-mediated gene transcription in the peri-infarct area after focal cerebral ischemia in mice. J Neurosci Res. 2004; 75:401–407. [PubMed: 14743453]

Swanson RA, Morton MT, Tsao-Wu G, Savalos RA, Davidson C, Sharp FR. A semiautomated method for measuring brain infarct volume. J Cereb Blood Flow Metab. 1990; 10:290–293. [PubMed: 1689322]

Tanaka K, Nagata E, Suzuki S, Dembo T, Nogawa S, Fukuuchi Y. Immunohistochemical analysis of cyclic AMP response element binding protein phosphorylation in focal cerebral ischemia in rats. Brain Res. 1999; 818:520–526. [PubMed: 10082840]

Zhang J, Li Y, Zhang ZG, Lu M, Borneman J, Buller B, Savant-Bhonsale S, Elias SB, Chopp M. Bone marrow stromal cells increase oligodendrogenesis after stroke. J Cereb Blood Flow Metab. 2009; 29:1166–1174. [PubMed: 19384336]

Zhang RL, Chopp M, Zhang ZG, Jiang Q, Ewing JR. A rat model of focal embolic cerebral ischemia. Brain Res. 1997; 766:83–92. [PubMed: 9359590]

Zhang ZG, Chopp M. Neurorestorative therapies for stroke: underlying mechanisms and translation to the clinic. Lancet Neurol. 2009; 8:491–500. [PubMed: 19375666]

Highlights

- Selective class IIa HDAC inhibition increases mortality and lesion volume.
- Selective class IIa HDAC inhibition impairs neuronal remodeling.
- Inactivation of CREB and c-fos likely contributes to this detrimental effect.
- Non-selective HDAC inhibition improves functional outcome after stroke.

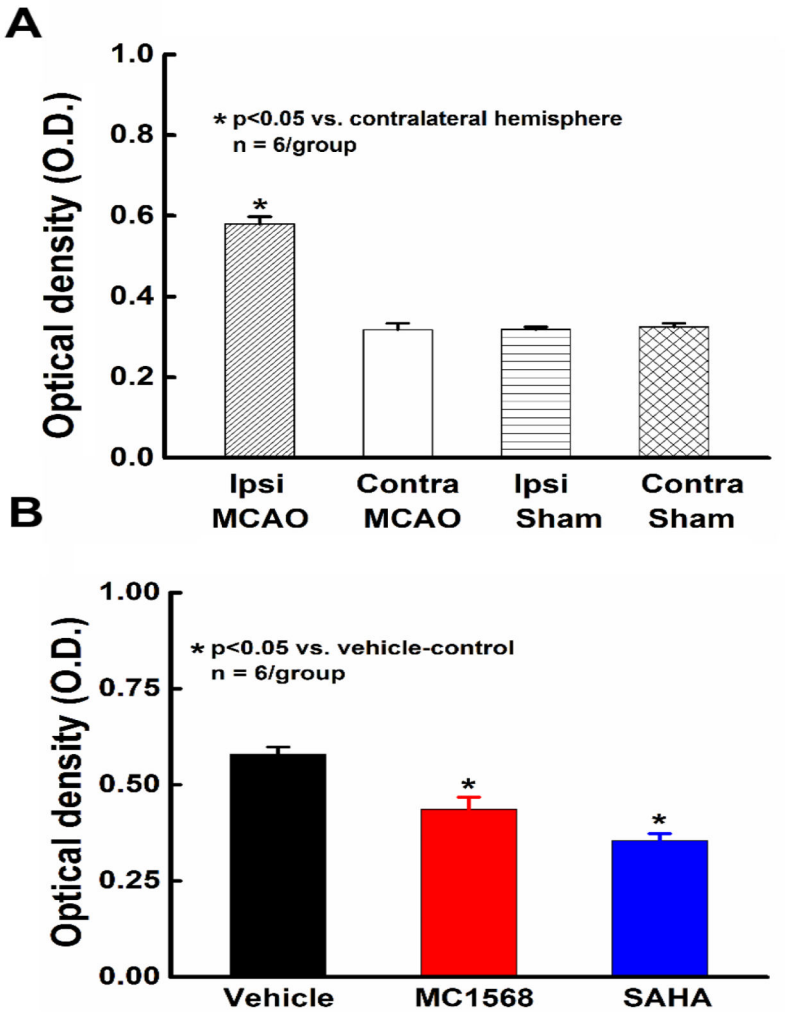

Figure 1.

Brain nuclear HDAC activity. Panels A and B show HDAC activity assessed in nuclear extracts of the contralateral and ipsilateral hemispheres of the brain from sham and vehicle-control ischemic rats 7 days after MCAO (**A**) and in nuclear extracts of the ipsilateral hemispheres of ischemic rats after treatments with vehicle, MC1568 and SAHA (**B**).

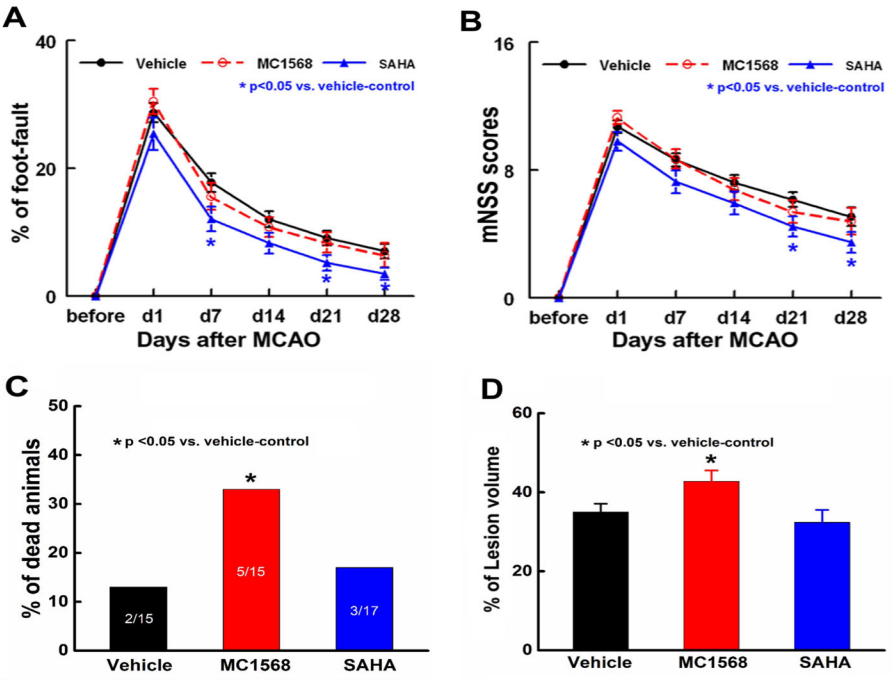

Figure 2.

The effect of HDAC inhibition on neurological outcomes after ischemic stroke. Panels A and B show foot-fault (**A**) and mNSS (**B**) test results during 28 days after MCAO (vehicle-control group n=13; MC1568 group n=10; SAHA group n=14). Panels C and D show mortality rate (**C**) and lesion volumes (**D**) in the three experimental groups after stroke.

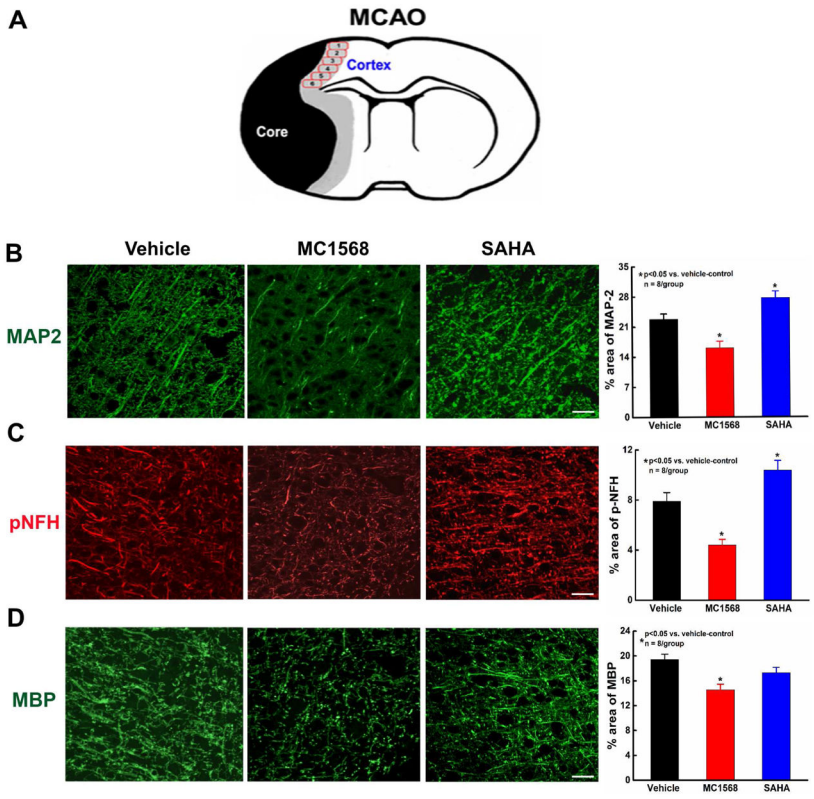

Figure 3.

The effect of HDAC inhibition on neurons and oligodendrocytes in ischemic brain. A schematic representation of a brain coronal section (**A**) shows that images were acquired from the peri-infarct cortex as outlined in the numbered boxes. Panels of B to D show confocal microscopic images of MAP2 (**B**), p-NFH (**C**) and MBP (**D**) immunoreactive neuronal and oligodendrocytes processes from representative animals and their corresponding quantitative data from animals treated with vehicle, MC1568 or SAHA 28 days after stroke. Bar = 20μm.

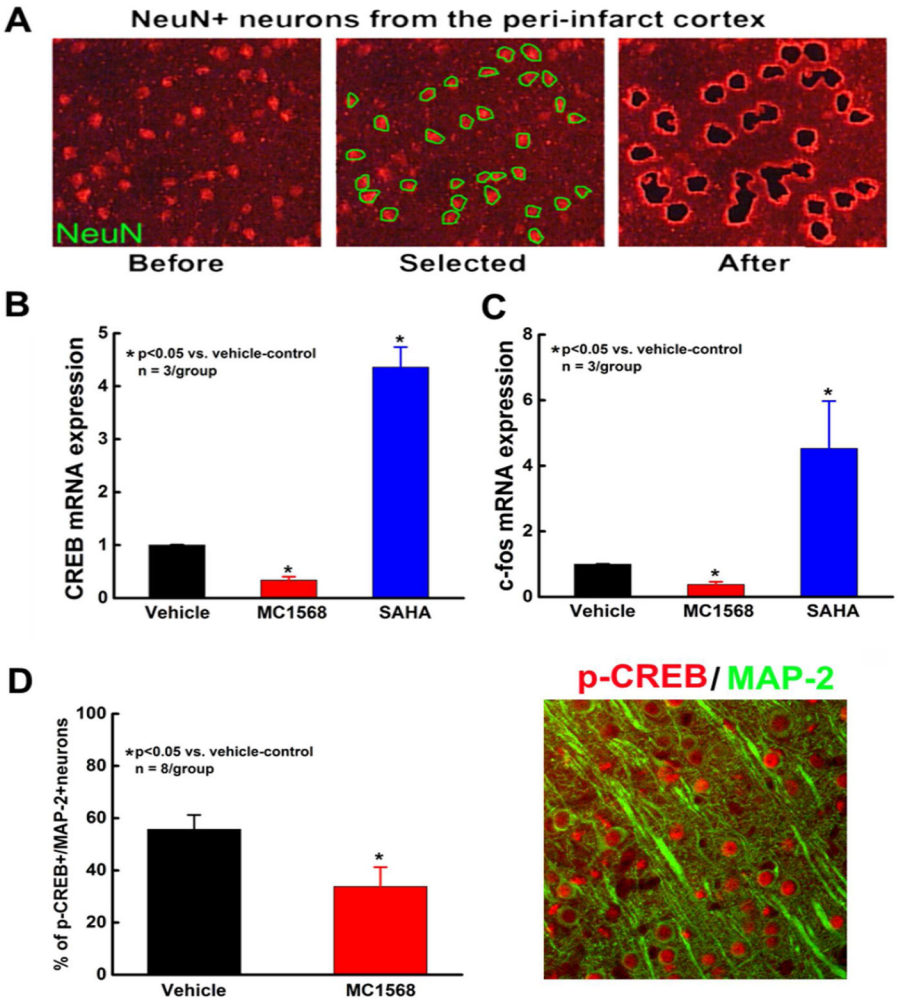

Figure 4.

The effect of HDAC inhibition on neuronal CREB and c-fos expression. Panel **A** shows fluorescent microscopic images of NeuN positive neurons localized to the peri-infarct cortex before and after LCM. Panels **B–C** show quantitative RT-PCR mRNA data of CREB (**B**) and c-fos (**C**) in cortical neurons acquired by LCM from rats treated with vehicle, MC1568 or SAHA. Panel **D** shows a representative double immunofluorescent image of phosphorylated CREB (p-CREB, red) and MAP2 (green) and quantitative data of p-CREB positive neurons in peri-infarct cortex of ischemic rats treated with vehicle or MC1568. Note: p-CREB immunoreactivity (red, arrows) was localized to nuclei of MAP2 positive neurons (green).